

# Adaptive Central-Upwind Schemes for Hamilton–Jacobi Equations with Nonconvex Hamiltonians

Alexander Kurganov<sup>1</sup> and Guergana Petrova<sup>2</sup>

*Received October 22, 2004; accepted (in revised form) October 14, 2005*

This paper is concerned with computing viscosity solutions of Hamilton–Jacobi equations using high-order Godunov-type projection-evolution methods. These schemes employ piecewise polynomial reconstructions, and it is a well-known fact that the use of more compressive limiters or higher-order polynomial pieces at the reconstruction step typically provides sharper resolution. We have observed, however, that in the case of nonconvex Hamiltonians, such reconstructions may lead to numerical approximations that converge to generalized solutions, different from the viscosity solution. In order to avoid this, we propose a simple adaptive strategy that allows to compute the unique viscosity solution with high resolution. The strategy is not tight to a particular numerical scheme. It is based on the idea that a more dissipative second-order reconstruction should be used near points where the Hamiltonian changes convexity (in order to guarantee convergence to the viscosity solution), while a higher order (more compressive) reconstruction may be used in the rest of the computational domain in order to provide a sharper resolution of the computed solution. We illustrate our adaptive strategy using a Godunov-type central-upwind scheme, the second-order generalized minmod and the fifth-order weighted essentially non-oscillatory (WENO) reconstruction. Our numerical examples demonstrate the robustness, reliability, and non-oscillatory nature of the proposed adaptive method.

**KEY WORDS:** Hamilton–Jacobi equations; nonconvex Hamiltonian; central-upwind schemes; generalized minmod limiter; WENO reconstruction.

<sup>1</sup> Mathematics Department, Tulane University, New Orleans, LA 70118, USA. E-mail: kurganov@math.tulane.edu

<sup>2</sup> Department of Mathematics, Texas A&M University, College Station, TX 77843, USA. E-mail: gpetrova@math.tamu.edu



28 **1. INTRODUCTION**

29 We study approximate solutions of the Hamilton–Jacobi (HJ) equation:

30 
$$\varphi_t + H(\nabla_{\mathbf{x}}\varphi) = 0, \quad \mathbf{x} \in \mathbb{R}^d, \quad (1.1)$$

31 computed using a class of projection-evolution methods, called Godunov-  
32 type schemes. One of the main building blocks of these schemes is a con-  
33 tinuous piecewise polynomial interpolant based on the point values of the  
34 computed solution. At every evolution step, this interpolant is evolved to  
35 the next time level according to (1.1). We have observed that, as in the  
36 case of nonconvex hyperbolic conservation laws (see [7]), the choice of the  
37 reconstruction is crucial for capturing the *viscosity solutions* of HJ equa-  
38 tions with nonconvex Hamiltonians (see [1, 11] and the references therein  
39 for a bird’s eye view on the theory of viscosity solutions and various  
40 applications). Namely, the use of a dissipative second-order reconstruction  
41 seems to result in the convergence of the computed solution toward the  
42 viscosity solution, while more compressive and higher-order reconstruc-  
43 tions may lead to the computation of a generalized solution, different  
44 from the viscosity solution. While this behavior is expected in the case  
45 of one-dimensional (1D) HJ equations (because of their direct relation  
46 to the corresponding scalar conservation laws and the results reported in  
47 [7]), it is completely new in the two-dimensional (2D) case, in which HJ  
48 equations and conservation laws are no longer equivalent. Notice that  
49 while dissipative reconstructions seem to ensure convergence to the phys-  
50 ically relevant solutions, higher-order (more compressive) reconstructions  
51 typically provide sharper resolution and a better quality of the computed  
52 solutions.

53 In this paper, we propose a simple adaptive strategy, which follows the  
54 one in [7] and automatically switches the high- and low-order reconstruc-  
55 tions around the points where the Hamiltonian changes convexity. This  
56 approach is not tight to a particular scheme and utilizes the advantages  
57 of both reconstructions in order to *compute the viscosity solution with high*  
58 *resolution*.

59 We illustrate this general strategy using a particular Godunov-  
60 type method—the central-upwind scheme from [2] with the dissipative  
61 second-order minmod reconstruction [8–10] and the fifth-order WENO  
62 reconstruction [3, 5]. The resulting method is referred to as *an adaptive semi-*  
63 *discrete central-upwind scheme*. However, we would like to point out once  
64 again that our adaptive strategy can be applied with any Godunov-type  
65 projection-evolution method and any couple of a dissipative and high-order  
66 (compressive) reconstructions.

67 The paper is organized as follows. In Sec. 2, we give a brief over-  
 68 view of the semi-discrete central-upwind schemes from [2] and describe our  
 69 adaptive strategy. The numerical experiments are carried out in Sec. 3.

## 70 2. SEMI-DISCRETE CENTRAL-UPWIND SCHEMES

### 71 2.1. Brief Overview

72 In this section, we describe the *low-dissipative semi-discrete second-*  
 73 *order central-upwind scheme* from [2] for the 1-D HJ equation:

$$74 \quad \varphi_t + H(\varphi_x) = 0, \quad x \in \mathbb{R}, \quad (2.1)$$

75 subject to the initial data  $\varphi(x, 0) = \varphi_0(x)$ . For simplicity, we consider a uni-  
 76 form grid in space and time, setting  $x_j := j\Delta x$  and  $t^n := n\Delta t$ . We denote  
 77 the approximate value of  $\varphi(x_j, t^n)$  by  $\varphi_j^n$  and assume that the values  $\varphi_j^n$   
 78 have been already computed. The solution at time  $t = t^n$  is then globally  
 79 approximated by a continuous non-oscillatory piecewise quadratic inter-  
 80 polant  $\tilde{\varphi}(x, t^n)$ , which is reconstructed from  $\varphi_j^n$ . At every grid point, the  
 81 maximal right and left speeds of propagation,  $a_j^+$  and  $a_j^-$  ( $a_j^\pm$  depend on  
 82 time,  $\varphi_x^\pm$  depend on both time and location, but these dependences are  
 83 omitted to simplify the notation), are estimated by

$$84 \quad \begin{aligned} a_j^+ &= \max_{\min\{\varphi_x^-, \varphi_x^+\} \leq u \leq \max\{\varphi_x^-, \varphi_x^+\}} \{H'(u), 0\}, \\ a_j^- &= \left| \min_{\min\{\varphi_x^-, \varphi_x^+\} \leq u \leq \max\{\varphi_x^-, \varphi_x^+\}} \{H'(u), 0\} \right|, \end{aligned} \quad (2.2)$$

85 where  $\varphi_x^\pm$  are the one-sided derivatives at  $x = x_j$ , that is,

$$86 \quad \varphi_x^\pm := \tilde{\varphi}_x(x_j \pm 0, t^n).$$

87 The values  $\varphi_x^\pm$  are given by:

$$88 \quad \varphi_x^\pm = \frac{(\Delta\varphi)_{j\pm\frac{1}{2}}^n}{\Delta x} \mp \frac{\Delta x}{2} (\varphi_{xx})_{j\pm\frac{1}{2}}^n, \quad (\Delta\varphi)_{j+\frac{1}{2}}^n := \varphi_{j+1}^n - \varphi_j^n, \quad (2.3)$$

89 where the second derivative is computed using a nonlinear limiter in order  
 90 to ensure a non-oscillatory nature of the reconstruction, and thus of the  
 91 resulting scheme. We use the generalized minmod limiter (see, e.g., [8–10])  
 92 to obtain

93

94

95

$$(\varphi_{xx})_{j+\frac{1}{2}}^n = \min\text{mod} \left( \theta \frac{(\Delta\varphi)_{j+\frac{3}{2}}^n - (\Delta\varphi)_{j+\frac{1}{2}}^n}{(\Delta x)^2}, \frac{(\Delta\varphi)_{j+\frac{3}{2}}^n - (\Delta\varphi)_{j-\frac{1}{2}}^n}{2(\Delta x)^2}, \right. \\ \left. \theta \frac{(\Delta\varphi)_{j+\frac{1}{2}}^n - (\Delta\varphi)_{j-\frac{1}{2}}^n}{(\Delta x)^2} \right). \quad (2.4)$$

96

In (2.4),  $\theta \in [1, 2]$  and the minmod function is given by

97

$$\min\text{mod}(x_1, x_2, \dots) := \begin{cases} \min_j \{x_j\}, & \text{if } x_j > 0 \quad \forall j, \\ \max_j \{x_j\}, & \text{if } x_j < 0 \quad \forall j, \\ 0, & \text{otherwise.} \end{cases}$$

98

It is well-known that larger values of  $\theta$  correspond to a less dissipative, more compressive reconstruction (see, e.g., [10]).

99

100

101

Finally, the semi-discrete central-upwind scheme from [2] can be written as the following system of ODEs:

102

103

$$\frac{d}{dt} \varphi_j(t) = - \frac{a_j^- H(\varphi_x^+) + a_j^+ H(\varphi_x^-)}{a_j^+ + a_j^-} \\ + a_j^+ a_j^- \left[ \frac{\varphi_x^+ - \varphi_x^-}{a_j^+ + a_j^-} - \min\text{mod} \left( \frac{\varphi_x^+ - \psi_x^{\text{int}}}{a_j^+ + a_j^-}, \frac{\psi_x^{\text{int}} - \varphi_x^-}{a_j^+ + a_j^-} \right) \right], \quad (2.5)$$

104

where  $\psi_x^{\text{int}}$  is given by

105

$$\psi_x^{\text{int}} := \frac{a_j^+ \varphi_x^+ + a_j^- \varphi_x^-}{(a_j^+ + a_j^-)} - \frac{H(\varphi_x^+) - H(\varphi_x^-)}{(a_j^+ + a_j^-)}. \quad (2.6)$$

106

107

108

109

The implementation of the semi-discrete scheme (2.2)–(2.6) requires a stable ODE solver of an appropriate order. In the numerical experiments, reported in Sec. 3, we have used the third-order strong stability preserving Runge–Kutta method [4].

110

111

112

For further details, we refer the reader to [2], where the central-upwind scheme (2.2)–(2.6) and its multidimensional and higher-order extensions are thoroughly described.

113

## 2.2. Adaption Algorithm

114

115

First, we will try to give some insight of the observed phenomenon. The problem is best understood in the 1D case, where differentiation of

116 the HJ equation (2.1) results in an equivalent scalar conservation law for  
 117  $\varphi_x$ . In the case of nonconvex  $H$ , the solution of the corresponding con-  
 118 servation law may develop composite waves that consist of a sequence  
 119 of joint rarefactions and shocks. The use of a low dissipative reconstruc-  
 120 tion, such as the second-order one based on the generalized minmod lim-  
 121 iter (2.4) with  $\theta = 2$  or the fifth-order WENO reconstruction, enhances  
 122 the influence of the shock over the rarefaction wave and thus leads to a  
 123 steeper piecewise polynomial reconstruction for  $\varphi_x$  in the neighborhoods  
 124 of shock-rarefaction junctions. The resulting overshoot/undershoot cannot  
 125 be compensated by the evolution (2.5), and leads to the computation of a  
 126 weak solution, different from the viscosity solution.

127 Next, we suggest an adaptive strategy that overcomes this difficulty:

- 128 • Use a second-order dissipative reconstruction at every point where  
 129 the convexity of the Hamiltonian changes and also within  $K$  neigh-  
 130 boring grid points (in the 2D case, this means  $K$  grid points in each  
 131 direction). At these grid points, the values of the local speeds are  
 132 calculated using (2.2).
- 133 • Use a high-order (compressive) reconstruction in the rest of the  
 134 computational domain, where (2.2) reduces to

$$135 \quad a_j^+ = \max \{H'(\varphi_x^-), H'(\varphi_x^+), 0\}, \quad a_j^- = |\min \{H'(\varphi_x^-), H'(\varphi_x^+), 0\}|.$$

### 136 **Remarks.**

- 137 1. Our numerical experiments suggest that in order to ensure conver-  
 138 gence to the viscosity solution,  $K$  should be taken proportional to  
 139  $|\ln(\Delta x)|$  as the grid is refined.
- 140 2. We denote by MM1 and MM2 the minmod limiter (2.4) with  $\theta =$   
 141 1 and  $\theta = 2$ , respectively, and by WENO5 the fifth-order WENO  
 142 reconstruction. In our numerical experiments, the adaption algo-  
 143 rithm has been realized using the MM1 as a dissipative recon-  
 144 struction and the WENO5 as a higher-order one.

## 145 **3. NUMERICAL EXAMPLES**

146 In this section, we illustrate the performance of our adaptive central-  
 147 upwind scheme. We show 2D examples only, since in the 1D case, the  
 148 differentiation of HJ equations results in equivalent scalar conservation  
 149 laws, for which the dependence of the computed solution on the recon-  
 150 struction has been discovered in [7].

151 As our 2-D numerical experiments suggest, the MM1 reconstruction  
 152 consistently leads to capturing the viscosity solution, while the use of  
 153 the MM2 or WENO5 reconstructions may or may not (depending on  
 154 the problem solved) lead to the convergence towards the viscosity solution.  
 155 The proposed adaptive scheme also consistently captures the viscosity  
 156 solution since our adaptive reconstruction reduces to the MM1 reconstruction  
 157 near the Hamiltonian inflection points. At the same time, it enjoys  
 158 high resolution property of the WENO5 reconstruction in the rest of the  
 159 computational domain. We would also like to point out that our adaptive  
 160 strategy does not seem to be very sensitive to the choice of adaption constant  
 161  $K$ . In the reported numerical examples,  $K=1$  in all  $201 \times 201$  computations,  
 162 while for the  $801 \times 801$  grid  $K=2$ .

163 **Example 1.** We numerically solve the 2D HJ equation:

$$164 \quad \varphi_t + \sin(\varphi_x) + \cos(\varphi_y) = 0, \quad (x, y) \in (-2, 2) \times (-2, 2), \quad t > 0, \quad (3.1)$$

165 subject to the following radially symmetric oscillatory initial condition  
 166  $\varphi(x, y, 0) = \varphi_0(r)$ ,  $r := \sqrt{x^2 + y^2}$ :

$$167 \quad \varphi_0(r) = \begin{cases} \frac{\pi}{4}(14r - 13), & r \leq \frac{1}{2}, \\ \frac{\pi}{4}(14r - 13) + 2 \sin(10\pi r), & \frac{1}{2} < r \leq 1, \\ \frac{\pi}{4}r, & r > 1, \end{cases} \quad (3.2)$$

168 and the homogeneous Neumann boundary conditions for  $\varphi_x$  and  $\varphi_y$ :

$$169 \quad \begin{cases} \varphi_{xx}(-2, y, t) = \varphi_{xx}(2, y, t) = 0, & \forall t, \forall y \in [-2, 2], \\ \varphi_{yy}(x, -2, t) = \varphi_{yy}(x, 2, t) = 0, & \forall t, \forall x \in [-2, 2]. \end{cases} \quad (3.3)$$

170 We have computed the solution of the initial-boundary-value (IBVP) problem  
 171 (3.1)–(3.3) at time  $t=2$  using the MM1, MM2, WENO5, and the  
 172 2D version of our adaptive reconstruction (we refer the reader to [2, 6,  
 173 8] for a detailed description of these 2D reconstructions). For adaption,  
 174 we check at every grid point whether a point where the convexity of the  
 175 Hamiltonian changes is near-by (in this example, the convexity changes at  
 176 the points where either  $\varphi_x = k\pi$  or  $\varphi_y = \ell\pi/2$ ,  $k, \ell \in \mathbb{Z}$ ). If this is the case,  
 177 that is, if the distance between the current grid point and one of the afore-  
 178 mentioned inflection points is smaller than  $K \max(\Delta x, \Delta y)$ , the dissipative  
 179 MM1 reconstruction is used at this grid point. Otherwise, the numerical  
 180 Hamiltonian there is computed using the sharper WENO5 reconstruction.

181 Even though the exact viscosity solution of this IBVP is unavailable,  
 182 it seems to be reasonable to expect that similarly to the case of hyper-  
 183 bolic conservation laws, studied in [7], the MM1 solution would capture  
 184 the viscosity solution. In Fig. 1, we show the solutions computed on a

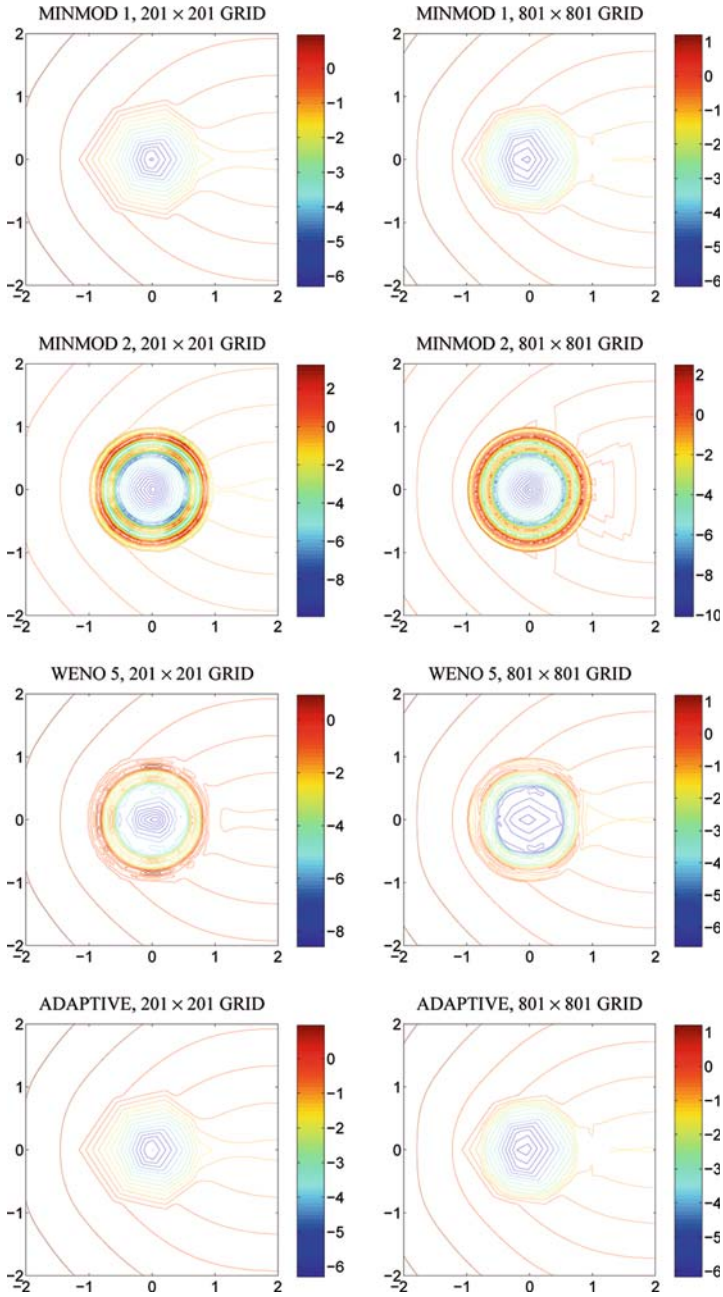


Fig. 1. Computed solutions of the IBVP (3.1)–(3.3).

185 relatively coarse  $201 \times 201$  grid and on a much finer  $801 \times 801$  grid. As one  
 186 can clearly see there, the difference between the MM1, MM2 and WENO5  
 187 solutions is quite significant (both MM2 and WENO5 solutions seem to  
 188 converge to generalized solutions, different from the viscosity solution).  
 189 On the other hand, both the MM1 solution and the solution, computed  
 190 by the adaptive central-upwind scheme, converge to what we believe to be  
 191 the viscosity solution of this IBVP.

192 The purpose of the next example is to show that even though both  
 193 the MM1 and adaptive solutions seem to converge to the viscosity solu-  
 194 tion, the adaptive solution provides higher resolution and thus justifies the  
 195 proposed adaptive strategy.

196 **Example 2.** We numerically solve a different 2D HJ equation:

$$197 \quad \varphi_t + \sin(\varphi_x) + \frac{1}{4}\varphi_y = 0, \quad (x, y) \in (-2, 2) \times (-2, 2), \quad t > 0, \quad (3.4)$$

198 subject to the same initial (3.2) and boundary (3.3) conditions. In this  
 199 example, the initial condition undergoes a nonlinear transformation in  
 200 the  $x$ -direction only, while it is being linearly advected in the  $y$ -direction.  
 201 Thus, the solution preserves some of its initial oscillatory nature, which is  
 202 captured much more accurately by a higher-order scheme.

203 As in Example 1, we compute the solution of the IBVP (3.2)–(3.4) at  
 204 time  $t = 2$  with  $201 \times 201$  and  $801 \times 801$  uniform grids using the MM1,  
 205 MM2, WENO5, and the adaptive reconstruction. The contour lines of  
 206 the computed solution, presented in Fig. 2, demonstrate the convergence  
 207 of both the MM1 and adaptive solutions to the viscosity solution. One  
 208 can only observe a superior resolution, achieved by the adaptive central-  
 209 upwind scheme due to the smaller amount of numerical viscosity. We  
 210 would like to mention that in this example, the WENO5 solution also  
 211 seems to converge to the viscosity solution though slower than its MM1  
 212 and adaptive counterparts. Also, notice that the WENO5 solution is much  
 213 more oscillatory than the MM1 and adaptive solutions.

214 The cross-sections at  $y = 0.5$  and  $x = 0$  of the MM1, WENO5 and  
 215 adaptive solutions, computed with the  $201 \times 201$  uniform grid are pre-  
 216 sented in Fig. 3. We also show the MM1 solution, computed on a finer  
 217  $801 \times 801$  grid, which serves as a reference solution. As one could expect,  
 218 the  $y = 0.5$  cross-sections of the MM1 and adaptive solutions are very  
 219 close (though the adaptive one is a little sharper near the extremum).  
 220 However, the  $x = 0$  cross-sections clearly demonstrate the advantage of the  
 221 proposed adaptive strategy: in the region where the solution has an oscil-  
 222 latory nature, the resolution achieved by the adaptive scheme with the  
 223  $201 \times 201$  grid seems to be superior to the one obtained by the second-  
 224 order MM1 scheme with the  $801 \times 801$  grid.

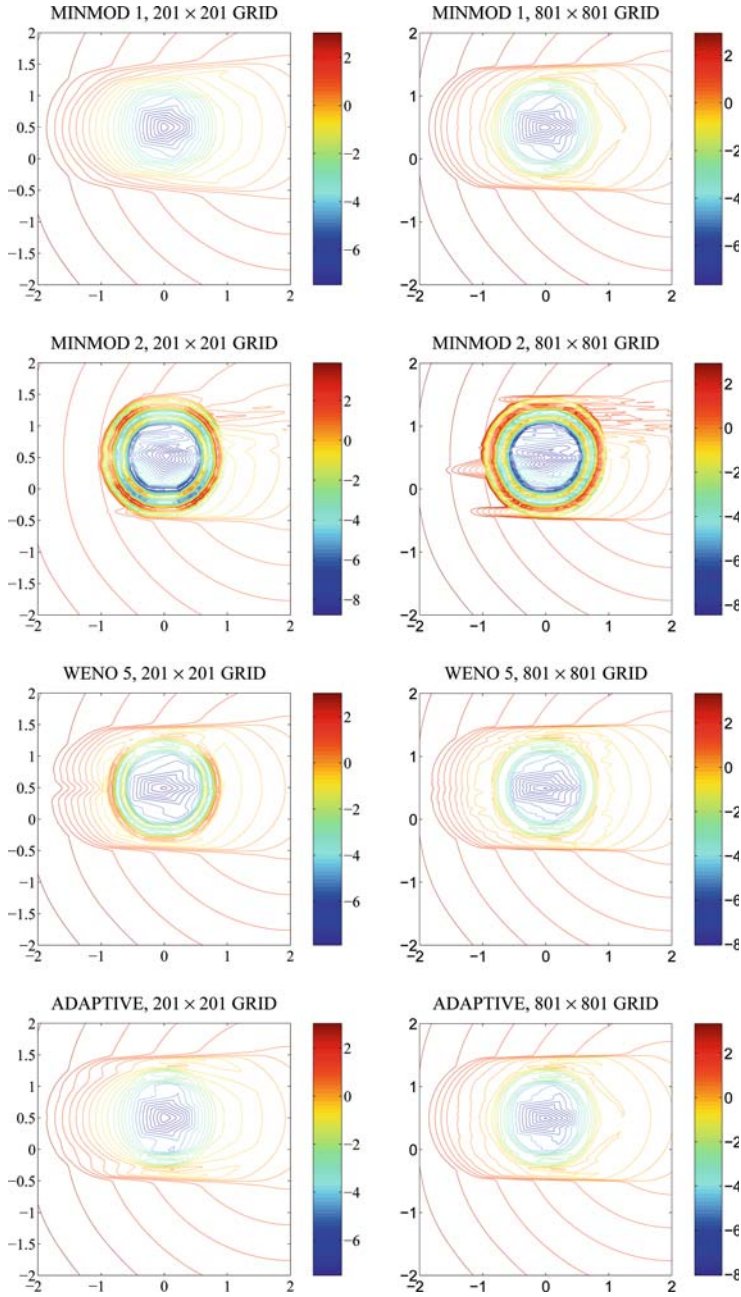


Fig. 2. Computed solutions of the IBVP (3.2)–(3.4).

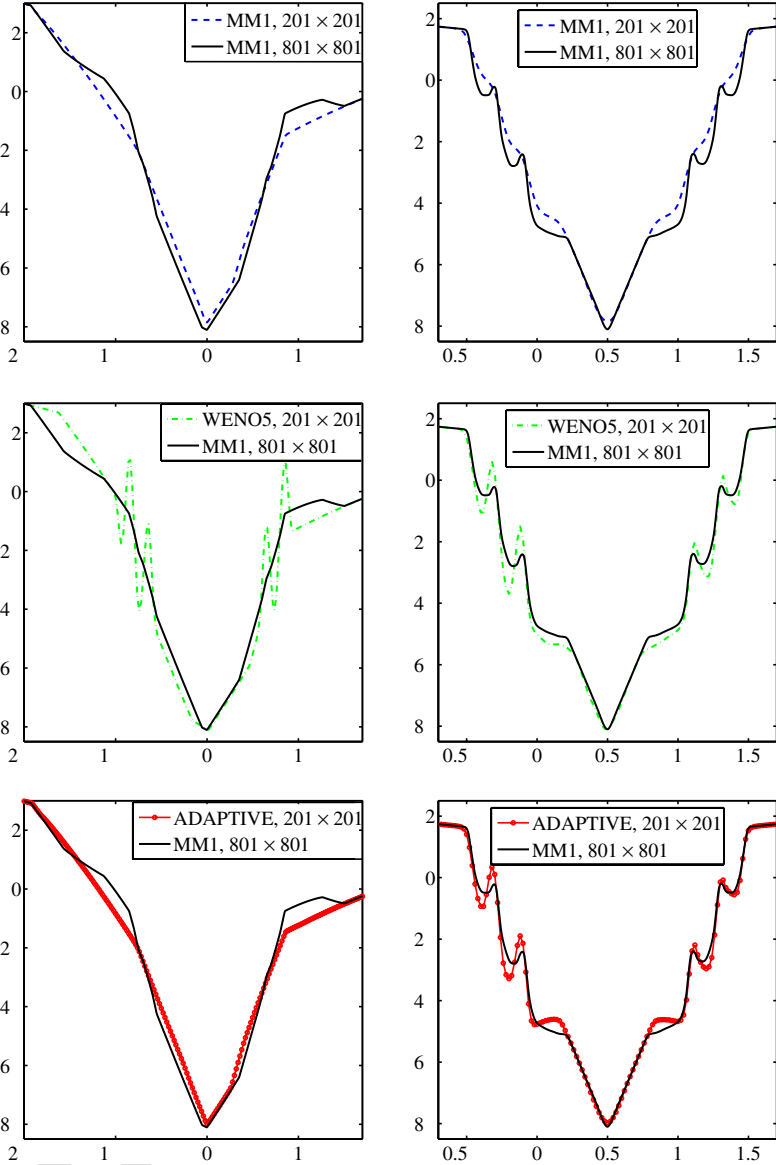


Fig. 3. Cross-sections at  $y = 0.5$  (left column) and  $x = 0$  (right column) of the MM1, WENO5, and adaptive solutions, computed on the  $201 \times 201$  grid, and the reference MM1 solution, computed on the  $801 \times 801$  grid.

225 **ACKNOWLEDGMENT**

226 The research of A. Kurganov was supported in part by the NSF  
227 Grant #DMS-0310585. The work of G. Petrova was supported in part by  
228 the NSF Grants #DMS-0296020 and #DMS-0505501.

229 **REFERENCES**

- 230 1. Bardi, M., Crandall, M., Evans, L., Sonar, H., and Souganidis, P. (1997). Viscosity  
231 solutions and applications. In Capuzzo Dolcetta, I. and Lions, P.-L. (eds.), Lecture  
232 Notes in Mathematics, Springer-Verlag, New York/Berlin, CIME Lecture Notes Vol.  
233 1660.
- 234 2. Bryson, S., Kurganov, A., Levy, D., and Petrova, G. (2005). Semi-discrete cen-  
235 tral-upwind schemes with reduced dissipation for Hamilton-Jacobi equations. *IMA*  
236 *J. Numer. Anal.* **25**, 113–138.
- 237 3. Bryson, S., and Levy, D., High-order semi-discrete central-upwind schemes for multi-  
238 dimensional Hamilton-Jacobi equations. *J. Comput. Phys.* **189**, 63–87.
- 239 4. Gottlieb, S., Shu, C.-W., and Tadmor, E. (2001). High order time discretization methods  
240 with the strong stability property. *SIAM Rev.* **43**, 89–112.
- 241 5. Jiang, G.-S., and Peng, D. (2000). Weighted ENO schemes for Hamilton-Jacobi equa-  
242 tions. *SIAM J. Sci. Comput.* **21**, 2126–2143.
- 243 6. Kurganov, A., Noelle, S., and Petrova, G. (2001). Semidiscrete central-upwind schemes  
244 for hyperbolic conservation laws and Hamilton-Jacobi equations. *SIAM J. Sci. Comput.*  
245 **23**, 707–740.
- 246 7. Kurganov, A., Petrova, G., and Popov, B. (submitted). Adaptive semi-discrete central-  
247 upwind schemes for nonconvex hyperbolic conservation laws. A preprint is available at  
248 <http://www.math.tulane.edu/~kurganov/pub.html>.
- 249 8. Kurganov, A., and Tadmor, E. (2000). New high-resolution semi-discrete schemes for  
250 Hamilton-Jacobi equations. *J. Comput. Phys.* **160**, 241–282.
- 251 9. van Leer, B. (1979). Towards the ultimate conservative difference scheme, V. A second  
252 order sequel to Godunov's method. *J. Comput. Phys.* **32**, 101–136.
- 253 10. Lie, K.-A., and Noelle, S. (2003). On the artificial compression method for second-order  
254 nonoscillatory central difference schemes for systems of conservation laws. *SIAM J. Sci.*  
255 *Comput.* **24**, 1157–1174.
- 256 11. Lions, P. (1982). Generalized solutions of Hamilton-Jacobi equations, Pitman Publishing  
257 Inc.